PHYSICAL REVIEW B **96**, 201115(R) (2017)

Interplay of charge and spin dynamics after an interaction quench in the Hubbard model

Marcin M. Wysokiński[1,2,*] and Michele Fabrizio[1,†]

[1]*International School for Advanced Studies (SISSA), via Bonomea 265, IT-34136 Trieste, Italy*

[2]*Marian Smoluchowski Institute of Physics, Jagiellonian University, ulica prof. S. Łojasiewicza 11, PL-30-348 Kraków, Poland*

(Received 9 October 2017; revised manuscript received 21 November 2017; published 30 November 2017)

We investigate the unitary dynamics following a sudden increase $\Delta U > 0$ of repulsion in the paramagnetic sector of the half-filled Hubbard model on a Bethe lattice, by means of a variational approach that combines a Gutzwiller wave function with a partial Schrieffer-Wolff transformation, both defined through time-dependent variational parameters. Besides recovering at ΔU_c the known dynamical transition linked to the equilibrium Mott transition, we find a pronounced dynamical anomaly at larger $\Delta U_* > \Delta U_c$ manifested in a singular behavior of the long-time average of double occupancy. Although the real-time dynamics of the variational parameters at ΔU_* strongly resembles the one at ΔU_c, a careful frequency spectrum analysis suggests a dynamical crossover, instead of a dynamical transition, separating regions of a different behavior of the spin exchange.

DOI: 10.1103/PhysRevB.96.201115

Pump-probe time-resolved spectroscopy is growing in importance as a tool for studying and manipulating correlated materials [1]. On one hand, it gives access to new enlightening information about the dynamical properties of those materials, beyond the reach of conventional spectroscopy. In addition, it provides a very efficient tool to drive phase transitions on ultrashort time scales, and concurrently investigate them in the time domain. There are cases where the photoinduced phases are actually those observed at thermal equilibrium upon heating, as, for instance, in photoexcited VO_2 [2]. This might be suggestive of a quasithermal pathway, though that is not generically the case, even in the same VO_2 [3]. Indeed, there is evidence of photoinduced hidden phases that are absent at equilibrium [4,5], as well as of remarkable nonthermal transient properties [6,7].

At first sight it might seem unsurprising to observe nonthermal behavior in correlated electron systems, which are complex materials with several competing phases and many actors playing a role. In reality, even the simplest among all models of correlated electrons, i.e., the single-band Hubbard model, where the complexity of real materials is reduced just to the competition between the on-site repulsion U and the nearest-neighbor hopping t, shows puzzling and still controversial nonthermal behavior. In a seminal work [8], Eckstein, Kollar, and Werner discovered by time-dependent dynamical mean-field theory (t-DMFT) that the unitary evolution of the half-filled Hubbard model in an infinitely coordinated Bethe lattice after a sudden increase of the repulsion U from the initial $U_0 = 0$ to a final $U_f > 0$ displays a sharp crossover at $U_f = U_c$, which, within the relatively short, numerically affordable simulation times, resembles a genuine dynamical transition. Such an interpretation was, however, contrasted by the observation that, if one assumes thermalization, the temperature that corresponds to the energy supplied by the quench $U = 0 \to U_c$ is well above the second-order critical end point of the Mott-transition line in the T vs U equilibrium phase diagram [8]. The same dynamical crossover was later found, still in an infinitely coordinated lattice, by a variational approach based on a time-dependent Gutzwiller wave function [9,10], which is not as rigorous as t-DMFT but allows simulating much longer times. In particular, by considering a linear ramp rather than a sudden quench, this crossover was shown [11] to be a genuine dynamical transition linked to the equilibrium Mott transition. The same conclusion has been recently drawn by the nonequilibrium self-energy functional theory [12], which is supposed to be more rigorous than the variational Gutzwiller approach, though not as much as t-DMFT. We emphasize that, should this dynamical anomaly be confirmed to correspond to a dynamical Mott transition, it would imply [8] that even the simplest single-band Hubbard model may display nonthermal behavior, at least in lattices with an infinite coordination number. However, there is evidence that the same occurs also when the coordination is finite [13,14].

It is therefore worth proving or disproving the existence of this dynamical transition by other complementary techniques, looking forward to numerical developments that could allow t-DMFT to finally settle this issue. Here, we make such an attempt by extending out of equilibrium the variational approach that we recently proposed [15], and which combines a Gutzwiller wave function with a partial Schrieffer-Wolff transformation, both defined now by time-dependent variational parameters. Although the method has the limits of any other variational approach, it does favorably benchmark [15] against more rigorous, but also numerically much more demanding, techniques.

We consider the half-filled single-band Hubbard model on an infinitely coordinated Bethe lattice,

$$H(t) = -\frac{1}{\sqrt{z}}\sum_{\langle ij\rangle} T_{\mathbf{ij}} + \frac{U(t)}{2}\sum_{\mathbf{i}}(n_{\mathbf{i}\uparrow} + n_{\mathbf{i}\downarrow} - 1)^2, \qquad (1)$$

where $z \to \infty$ is the coordination number, $U(t)$ the time-dependent on-site repulsion, $U(t < 0) = U_0$ and $U(t \geqslant 0) = U_f$, and $T_{\mathbf{ij}} \equiv \sum_\sigma (c^\dagger_{\mathbf{i}\sigma} c_{\mathbf{j}\sigma} + \text{H.c.})$ the hopping operator on the bond $\langle ij\rangle$ connecting the nearest-neighbor sites i and j.

The dynamics of the model is determined through the saddle point of the action

$$\mathcal{S} = \int dt\, \langle\Psi(t)|i\frac{d}{dt} - H(t)|\Psi(t)\rangle, \qquad (2)$$

*mwysoki@sissa.it
†fabrizio@sissa.it

which provides the exact solution of the Schrödinger equation for unrestricted many-body wave functions $\Psi(t)$, or just a variational estimate of it in case $\Psi(t)$ varies within a subspace of the whole Hilbert space, which is what we shall do hereafter. In particular, we assume for $\Psi(t)$ the expression [15]

$$|\Psi(t)\rangle = \mathcal{U}(t)\mathcal{P}_G(t)|\psi_0(t)\rangle, \tag{3}$$

where $\psi_0(t)$ is a paramagnetic uniform Slater determinant, $\mathcal{U}(t)$ a unitary transformation, and finally $\mathcal{P}_G(t) \equiv \prod_{\mathbf{i}} \mathcal{P}_{\mathbf{i}}(t)$, with $\mathcal{P}_{\mathbf{i}}(t)$ a linear operator on the local Hilbert space [9]. In the presence of particle-hole symmetry and discarding the spontaneous breakdown of spin SU(2) symmetry, $\mathcal{P}_{\mathbf{i}}(t)$ can be generically written as

$$\mathcal{P}_{\mathbf{i}}(t) = \sqrt{2}\,\phi_{\mathbf{i}0}(t)[\mathrm{P}_{\mathbf{i}}(0) + \mathrm{P}_{\mathbf{i}}(2)] + \sqrt{2}\,\phi_{\mathbf{i}1}(t)\mathrm{P}_{\mathbf{i}}(1), \tag{4}$$

where $\mathrm{P}_{\mathbf{i}}(n)$ is the projection operator at site i onto the configuration with n electrons, whereas $\phi_{\mathbf{i}n}(t)$ is a complex function of time [9]. In infinitely coordinated lattices the wave function $|\Psi(t)\rangle$ is normalized at any time if $|\phi_{\mathbf{i}0}(t)|^2 + |\phi_{\mathbf{i}1}(t)|^2 = 1$.

The time-dependent unitary transformation $\mathcal{U}(t)$ is of the Schrieffer-Wolff type [15–17], and it is parametrized by complex, time, and bond-dependent variational parameters $\epsilon_{\mathbf{ij}}(t)$,

$$\mathcal{U}(t) \equiv e^{A(t)} \equiv \exp\left[\frac{1}{\sqrt{z}}\sum_{\langle\mathbf{ij}\rangle}[\epsilon_{\mathbf{ij}}(t)\tilde{T}_{\mathbf{ij}} - \epsilon^*_{\mathbf{ij}}(t)\tilde{T}^\dagger_{\mathbf{ij}}]\right], \tag{5}$$

where

$$\begin{aligned}\tilde{T}_{\mathbf{ij}} &\equiv [\mathrm{P}_{\mathbf{i}}(2)\mathrm{P}_{\mathbf{j}}(0) + \mathrm{P}_{\mathbf{i}}(0)\mathrm{P}_{\mathbf{j}}(2)]T_{\mathbf{ij}}[\mathrm{P}_{\mathbf{i}}(1)\mathrm{P}_{\mathbf{j}}(1)],\\ \tilde{T}^\dagger_{\mathbf{ij}} &\equiv [\mathrm{P}_{\mathbf{i}}(1)\mathrm{P}_{\mathbf{j}}(1)]T_{\mathbf{ij}}[\mathrm{P}_{\mathbf{i}}(2)\mathrm{P}_{\mathbf{j}}(0) + \mathrm{P}_{\mathbf{i}}(0)\mathrm{P}_{\mathbf{j}}(2)],\end{aligned} \tag{6}$$

are the components of the hopping operator T_{ij} that couple the low-energy subspace of singly occupied sites i and j with the high-energy one where one site is empty and the other doubly occupied.

We determine $\psi_0(t)$, $\mathcal{P}_G(t)$, and $\mathcal{U}(t)$ through the saddle point of the action (2) with respect to all the variational parameters, handling $\mathcal{U}(t)$ by a series expansion

$$\mathcal{U}^\dagger O \mathcal{U} = O - [A, O] + \tfrac{1}{2}[A,[A,O]] + \cdots, \tag{7}$$

up to the desired order. For instance,

$$\begin{aligned}\mathcal{U}^\dagger H \mathcal{U} \simeq H &+ \frac{U}{\sqrt{z}}\sum_{\mathbf{ij}}(\epsilon_{\mathbf{ij}}\tilde{T}_{\mathbf{ij}} + \epsilon^*_{\mathbf{ij}}\tilde{T}^\dagger_{\mathbf{ij}})\\ &+ \frac{1}{8z}\sum_{\mathbf{ij}} J_{\mathbf{ij}}[\tilde{T}_{\mathbf{ij}} + \tilde{T}^\dagger_{\mathbf{ij}}, \tilde{T}_{\mathbf{ij}} - \tilde{T}^\dagger_{\mathbf{ij}}] + H_{\mathcal{R}},\end{aligned} \tag{8}$$

where

$$J_{\mathbf{ij}} = 4[(\epsilon_{\mathbf{ij}} + \epsilon^*_{\mathbf{ij}})V - U|\epsilon_{\mathbf{ij}}|^2], \tag{9}$$

and higher-order terms are stored together in $H_{\mathcal{R}}$. In the calculation below we stop the series expansion at the third order in power of ϵ, and consider all processes up to three neighboring sites. We have tested such an approximation at equilibrium in comparison with exact DMFT results [18], and it provides a quite satisfactory description of the metal and insulating phases for $U \gtrsim U_{\mathrm{Mott}}/2$, where U_{Mott} is the equilibrium location of the Mott transition (cf. Supplemental Material, Sec. I [19]). Inclusion of higher orders systematically increases the accuracy and thus allows accessing also the weaker correlated regime [15]. However, for the sake of simplicity, we decided to stand to the above approximation, and consequently we just considered quantum quenches from a relatively correlated metal at $U_0 > U_{\mathrm{Mott}}/2$ to higher values of $U_f > U_0$.

With this prescription for handling the unitary operator $\mathcal{U}(t)$, the expectation values that define the action (2) can be explicitly evaluated when the coordination number $z \to \infty$, and can be formally written as

$$\begin{aligned}\langle\Psi|i\frac{d}{dt}|\Psi\rangle &= i\langle\psi_0|\dot{\psi}_0\rangle + i\sum_{\mathbf{i}}(\phi^*_{\mathbf{i}1}\dot{\phi}_{\mathbf{i}1} + \phi^*_{\mathbf{i}0}\dot{\phi}_{\mathbf{i}0})\\ &\quad + if(\mathbf{v}, \dot{\epsilon}_{\mathbf{ij}}, \dot{\epsilon}^*_{\mathbf{ij}}, \psi_0, \psi^*_0),\end{aligned} \tag{10}$$

$$\langle\Psi|H|\Psi\rangle = h(\mathbf{v}, \psi_0, \psi^*_0), \tag{11}$$

where $\mathbf{v} = \{\phi_{\mathbf{i}0}, \phi^*_{\mathbf{i}0}, \phi_{\mathbf{i}1}, \phi^*_{\mathbf{i}1}, \epsilon_{\mathbf{ij}}, \epsilon^*_{\mathbf{ij}}\}$. Being too lengthy, the actual expressions of the functions f and h are given in the Supplemental Material, Sec. II [19].

The saddle-point equations that determine the evolution of the wave function can be readily obtained. As in the time-dependent Gutzwiller approximation [9], the evolution of the Slater determinant $\psi_0(t)$ is trivially just the multiplication by a time-dependent phase, so that, for instance, $\langle\psi_0(t)|\frac{1}{\sqrt{z}}\sum_{ij} T_{\mathbf{ij}}|\psi_0(t)\rangle = 8/3\pi \equiv T_0$ is time independent. In what follows, we shall use as the energy unit $8T_0$, and define $u = U/8T_0$. In these units, the initial state is always prepared at $u_0 = 0.5$ and then instantly quenched to the final value $u_f > 0.5$.

On the contrary, the Euler-Lagrange equations for the components of the variational parameter $\mathbf{v}$ are not trivial and read

$$\begin{aligned}i\dot{\phi}_{\mathbf{i}0} + i\frac{\partial f}{\partial \phi^*_{\mathbf{i}0}} - \frac{\partial h}{\partial \phi^*_{\mathbf{i}0}} &= 0,\\ i\dot{\phi}_{\mathbf{i}1} + i\frac{\partial f}{\partial \phi^*_{\mathbf{i}1}} - \frac{\partial h}{\partial \phi^*_{\mathbf{i}1}} &= 0,\\ i\frac{\partial f}{\partial \epsilon_{\mathbf{ij}}} - \frac{\partial h}{\partial \epsilon_{\mathbf{ij}}} - i\frac{d}{dt}\frac{\partial f}{\partial \dot{\epsilon}_{\mathbf{ij}}} &= 0,\end{aligned} \tag{12}$$

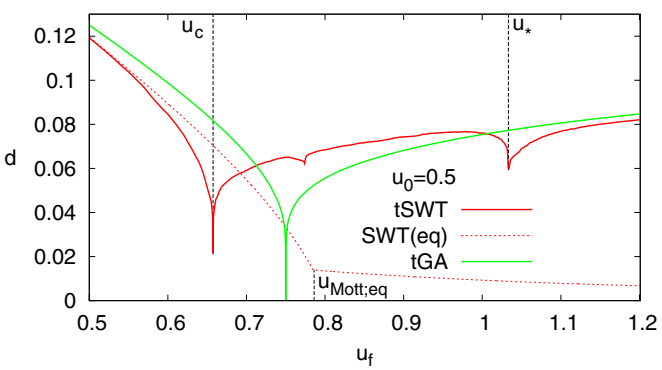

FIG. 1. Average double occupancy after the quench from the correlated metal at $u_0 = 0.5$. For the sake of completeness, we also show the equilibrium result of a Gutzwiller wavefunction combined with a Schrieffer-Wolff transformation (SWT) [15] as well as that obtained by the simpler time-dependent Gutzwiller wave function (tGA) [9].

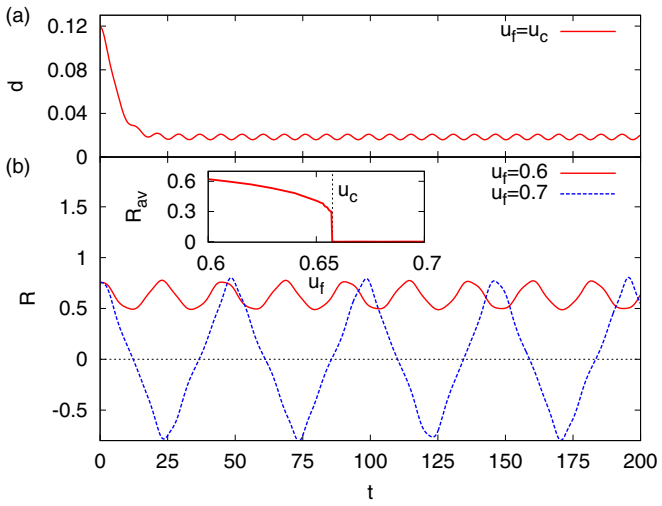

FIG. 2. (a) Time evolution of the double occupancy $d(t)$ at u_c. (b) Time evolution of $R(t)$ just before and after u_c, with its time average drawn in the inset. We note that indeed R has a critical behavior at u_c.

plus their complex conjugates. Assuming translational invariance, we can discard the site index in the above equations. The resulting differential equations are lengthy but can be written in the following matrix form,

$$\hat{B}[\mathbf{v}(t)]\dot{\mathbf{v}}(t) = \mathbf{a}[\mathbf{v}(t)], \tag{13}$$

i.e., as a set of ordinary first-order nonlinear differential equations, which can be numerically integrated by Runge-Kutta types of algorithms (see Supplemental Material, Sec. III [19]).

In Fig. 1 we plot the long-time average of the double occupancy per site. At $u_c \simeq 0.6575$ we observe a first dynamical anomaly, which is actually the already known *dynamical transition* [8,9,12] at which the system shows a rapid relaxation to a Mott insulator [cf. Fig. 2(a)]. Within Gutzwiller types of wave functions, the Mott transition is characterized by an order parameter $R = \phi_0\phi_1^* + \phi_1\phi_0^*$, which is finite in the metal and vanishes in the insulator [9,20]. Formally, R is defined by observing that the action of the projected operator $\mathcal{P}_i^\dagger c_{i\sigma}\mathcal{P}_i$ on the Slater determinant ψ_0 is the same as $Rc_{i\sigma}$, so that R can be regarded as the quasiparticle component in the physical electron $c_{i\sigma}$. In Fig. 2(b) we show that, for $u_f < u_c$, $R(t)$ oscillates around a finite value, whereas above u_c it oscillates around zero, as clear in the inset where its time average is plotted. Therefore our improved wave function also points to a genuine dynamical Mott transition occurring at u_c, which, as we mentioned, contrasts the belief that the system thermalizes.

In addition, we note two further dynamical anomalies at $u_f \simeq 0.77$ and $u_f = u_* \simeq 1.0326$, the latter more pronounced. To better explore their nature, in Fig. 3 we draw the frequency spectra of $R(t)$ and of the real part of $\epsilon(t)$, which show that both anomalies are actually triggered by the frequency crossing of different modes. In addition, at u_* there is also one mode that gets soft, not much different from what happens at u_c. In order to identify the origin of the different modes and the meaning of the softening, we compare the frequency spectrum of $R(t)$ with the corresponding one in the simpler time-dependent Gutzwiller wave function [9] (see Sec. IV of the Supplemental Material [19]), which lacks the spin correlations brought by the Schrieffer-Wolff transformation. Both spectra have in common the mode with frequency ω_H [see Fig. 3(a)]. We thus conclude that ω_H originates solely from the dynamics of charge degrees of freedom, and can be associated with the *Hubbard-band mode* discussed in Ref. [21] that becomes soft at the equilibrium Mott transition. In the present nonequilibrium condition, the softening of the same mode and its higher harmonics is further confirmation that u_c signals a genuine dynamical Mott transition.

On the other hand, the Schrieffer-Wolff transformation leads to the appearance of a new mode that does not soften at u_c, and which we associate with the spin exchange J of Eq. (9) and thus denote as exchange mode ω_J, marked with a blue dashed line in Fig. 3.

We have found that all remaining frequencies in Fig. 3(a) are quantized linear combinations of the two principal frequencies ω_H and ω_J, as expected because of the nonlinear character of the Euler-Lagrange equations (13). We shall label those secondary frequencies by two integers n,k, and denote them as $\omega_{n,k}$ for $u_f < u_c$, while, above u_c, as $\Omega_{n,k}$ and $\Omega'_{n,k}$, in the power spectra of $R(t)$ [Fig. 3(a)] and $\epsilon(t)$ [Fig. 3(b)], respectively. These frequencies are constructed according to

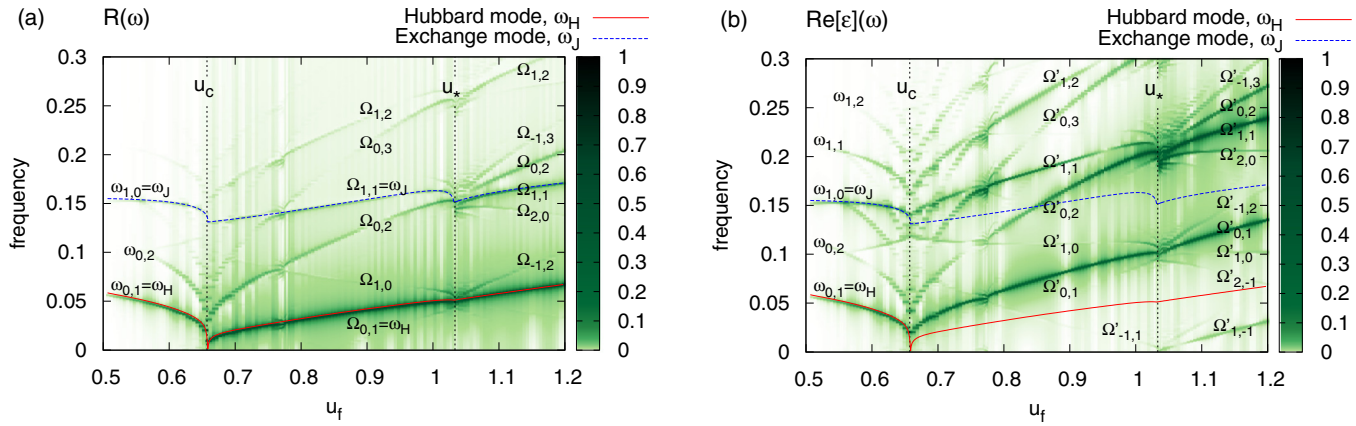

FIG. 3. Frequency spectra of $R(t)$, i.e., the real part of $\phi_0\phi_1^*$, and of the real part of ϵ, (a) and (b), respectively. The meaning of the frequency labels is explained in the main text.

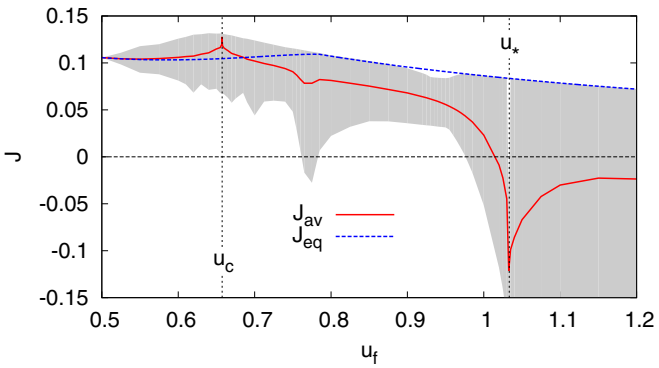

FIG. 4. Red solid line: Time average value $J_{\rm av}$ of $J(t)$ in Eq. (9), as a function of u_f. Blue dashed line: The value $J_{\rm eq}$ of J obtained at equilibrium by minimizing the energy at $u = u_f$. In gray, we indicate the region covered by the time fluctuations of $J(t)$.

the following rules:

$$\begin{aligned} \omega_{n,k} &= n\omega_J + k\omega_H, \\ \Omega_{n,k} &= n(\omega_J - \omega_H) + (2k-1)\omega_H, \\ \Omega'_{n,k} &= \Omega_{n,k} + \omega_H = n(\omega_J - \omega_H) + 2k\omega_H. \end{aligned} \tag{14}$$

Without the Schrieffer-Wolff transformation, i.e., with $\omega_J = 0$, the above rules easily follow from the equations of motion of a classical pendulum that control the dynamics of the simple time-dependent Gutzwiller wave function [9]. On the contrary, we determined empirically the rules (15) when $\omega_J \neq 0$.

According to the rules (15), mode crossings occur whenever $\omega_J = (2m+1)\omega_H$, and thus the anomaly at $u_f \simeq 0.77$ corresponds to $m = 2$ while that at u_* to $m = 1$. Moreover, the apparent softening in the dynamics of ϵ is in reality the vanishing of the linear combination $\Omega'_{\pm 1,\mp 1}$. In other words, the anomaly at u_* is not characterized by the softening of any of the principal modes, ω_H or ω_J, and therefore it is not to be confused with a genuine dynamical transition. Nonetheless, close to u_*, we do find changes in the physical properties. In Fig. 4 we plot as a function of u_f the time average $J_{\rm av}$ of the spin exchange $J(t)$ in Eq. (9), the region covered by its time fluctuations, as well as its equilibrium value $J_{\rm eq}$. We observe that, just before u_*, $J_{\rm av}$ turns from antiferromagnetic to ferromagnetic and its fluctuations grow larger, which suggests a change in character of the spin correlations. Indeed, in our variational approach the sign change of $J_{\rm av}$ is a simple way to compensate for the antiferromagnetic correlations built into the uncorrelated Slater determinant $|\psi_0(t)\rangle$ in Eq. (3), and thus to absorb part of the excess energy supplied by the quench. We also argue it might correspond to the melting of antiferromagnetism that should occur when suddenly increasing U starting from a Néel ordered state [22].

In summary, we have studied the quench dynamics in the paramagnetic sector of the half-filled single-band Hubbard model on an infinitely coordinated Bethe lattice, by means of a variational Gutzwiller wave function enriched with spin correlations by a variational Schrieffer-Wolff transformation. We have confirmed the existence of a dynamical Mott transition at odds with the belief that the model should finally relax to a thermal state. Even though the variational wave function does not allow for all dissipative channels that exist in the real time evolution, we nonetheless believe that the softening of the Hubbard-band mode with frequency ω_H, which signals the Mott transition at equilibrium [21], is a genuine phenomenon that will not be swept out in more rigorous calculations. In addition, we have found that the time-dependent Schrieffer-Wolff transformation yields nontrivial spin correlations that undergo a dynamical change for a final interaction value quite beyond the dynamical Mott transition.

M.M.W. acknowledges support from the Polish Ministry of Science and Higher Education under the "Mobility Plus" programme, Agreement No. 1265/MOB/IV/2015/0, as well as from the Foundation for Polish Science under the "START" programme. M.F. acknowledges support from European Union under the H2020 Framework Programme, ERC Advanced Grant No. 692670 "FIRSTORM".

[1] C. Giannetti, M. Capone, D. Fausti, M. Fabrizio, F. Parmigiani, and D. Mihailovic, Adv. Phys. **65**, 58 (2016).
[2] A. Cavalleri, C. Tóth, C. W. Siders, J. A. Squier, F. Ráksi, P. Forget, and J. C. Kieffer, Phys. Rev. Lett. **87**, 237401 (2001).
[3] B. Mayer, C. Schmidt, A. Grupp, J. Bühler, J. Oelmann, R. E. Marvel, R. F. Haglund, T. Oka, D. Brida, A. Leitenstorfer *et al.*, Phys. Rev. B **91**, 235113 (2015).
[4] L. Stojchevska, I. Vaskivskyi, T. Mertelj, P. Kusar, D. Svetin, S. Brazovskii, and D. Mihailovic, Science **344**, 177 (2014).
[5] J. Zhang, X. Tan, M. Liu, S. W. Teitelbaum, K. W. Post, F. Jin, K. A. Nelson, D. N. Basov, W. Wu, and R. D. Averitt, Nat. Mater. **15**, 956 (2016).
[6] D. Fausti, R. I. Tobey, N. Dean, S. Kaiser, A. Dienst, M. C. Hoffmann, S. Pyon, T. Takayama, H. Takagi, and A. Cavalleri, Science **331**, 189 (2011).
[7] M. Mitrano, A. Cantaluppi, D. Nicoletti, S. Kaiser, A. Perucchi, S. Lupi, P. Di Pietro, D. Pontiroli, M. Ricc, S. R. Clark *et al.*, Nature (London) **530**, 461 (2016).
[8] M. Eckstein, M. Kollar, and P. Werner, Phys. Rev. Lett. **103**, 056403 (2009).
[9] M. Schiró and M. Fabrizio, Phys. Rev. Lett. **105**, 076401 (2010).
[10] M. Schiró and M. Fabrizio, Phys. Rev. B **83**, 165105 (2011).
[11] M. Sandri, M. Schiró, and M. Fabrizio, Phys. Rev. B **86**, 075122 (2012).
[12] F. Hofmann, M. Eckstein, and M. Potthoff, Phys. Rev. B **93**, 235104 (2016).
[13] S. A. Hamerla and G. S. Uhrig, Phys. Rev. B **87**, 064304 (2013).
[14] S. A. Hamerla and G. S. Uhrig, Phys. Rev. B **89**, 104301 (2014).

[15] M. M. Wysokiński and M. Fabrizio, Phys. Rev. B **95**, 161106(R) (2017).
[16] K. A. Chao, J. Spałek, and A. M. Oleś, J. Phys. C **10**, L271 (1977).
[17] M. Eckstein, J. H. Mentink, and P. Werner, arXiv:1703.03269.
[18] C. Weber, A. Amaricci, M. Capone, and P. B. Littlewood, Phys. Rev. B **86**, 115136 (2012).
[19] See Supplemental Material at http://link.aps.org/supplemental/10.1103/PhysRevB.96.201115 for details of implementation of the method and its comparison to other theoretical approaches.
[20] R. Žitko and M. Fabrizio, Phys. Rev. B **91**, 245130 (2015).
[21] M. Fabrizio, Phys. Rev. B **95**, 075156 (2017).
[22] M. Sandri and M. Fabrizio, Phys. Rev. B **88**, 165113 (2013).